Numerical analysis of thermal stress in laser cladding technology of M4 High Speed Steel

R. T. Jardin[1], J. Tchoufang Tchuindjang[2], L. Duchêne[1], R. Carrus[3], A. Mertens[2], A. M. Habraken*[1], H-S Tran[1]

[1]University of Liege, MSM Unit, Allée de la Découverte, 9 B52/3, B 4000 Liège, Belgium
[2]University of Liege, MMS Unit, Allée de la Découverte, 9 B52/3, B 4000 Liège, Belgium
[3]Sirris Research Centre (Liège), Rue Bois St-Jean, 12, B 4102 Seraing, Belgium
*Corresponding Author A.M. Habraken (Anne.Habraken@uliege.be)

Keywords: Finite Element, Experimental Validation, Thermomechanical Analysis

Abstract

Directed Energy Deposition also called laser cladding process involves high thermal gradients resulting in important stress fields, distortions and possibly cracks. Using the academic non-linear finite element code LAGAMINE developed by Uliege, fully coupled thermo-mechanical simulations of laser cladding process of a thin wall in High Speed Steel are performed. A thermo-elasto-plastic constitutive law is used. The thermal model is validated by comparisons between predicted and measured substrate temperatures. The sensitivity of the predicted stresses to the use of simple or multilinear hardening law coupled or not to numerical annealing temperature is demonstrated.

1. Introduction

High Speed Steels (HSS) are widely used in various applications including cutting operations, high speed machining, hot stamping, moulding and hot strip mills. These alloys belong to the complex Fe-Cr-C-X system, where X is a strong carbide-forming element such as V, Nb, Mo or W. The carbide content improves the mechanical properties as well as the wear and oxidation resistance [1]. Laser cladding process is advantageously used as a repair technology, production of functional prototypes or small series. However some problems are still to be mastered, such as microstructure monitoring, geometry accuracy, and crack events during manufacturing.

The melt pool size has been identified as a critical parameter for maintaining optimal built conditions [2]. For instance, [3] provides process maps (absorbed power and beam velocity related to constant melt pool area) for controlling solidification microstructure (grain size, fully columnar, fully equiaxed, mix). Such guidance for optimal process parameters heavily relies on finite element (FE) simulations. While the preheating temperature is studied by [4] for Ti-6Al-4V, [5] is focused on bulk M4 HSS samples. It links the thermal field history and the generated microstructures.

However previous works do not discuss the impact on the FE thermal predictions of the accuracy of the input material data. Regularly missing material data justifies the use of temperature-independent thermo-physical properties [6].Other issues are related to the impact of boundary conditions (convection, radiation coefficient) on the FE results as

pointed by [7] where a distribution function of the heat convection coefficients at the thin wall and substrate surface is applied. Hereafter, the use of constant values of convection, radiation coefficients allows to recover the temperature measurements.

FE thermo-mechanical simulations provide the history of stress fields allowing crack prediction during the process and residual stress in the final part. However they need material parameters such as dilatation coefficient, Young modulus depending on temperature, tensile stress-strain curves at different strain rates and temperatures. Hereafter, 3D FE simulations of thin wall experiments are described. Local temperatures measured during the process allow a first validation. The well-known concept of numerical annealing temperature [8] from welding models is naturally applied here as in [9] while other authors [10] do not use it. It seems physically consistent to forget any plastic strain performed at higher temperature than a well chosen annealing temperature. However the sensitivity of the predicted stresses to this temperature choice depends on the hardness slope as shown hereafter.

2. Experiments

HSS M4 commercial powder (see [5]) with particle size ranging from 50 µm to 150 µm generates thin wall samples. The 5-axis Irepa Laser Cladding system with a Nd-YAG laser of maximum power capacity of 2000 W from Sirris Research Centre is used. This laser has a wavelength of 1064 µm and operates continuously. The laser has a top-hat energy distribution with a diameter of 1400 µm. The substrate consists in a small rectangular bar of 8 mm height, 10 mm width and 120 mm length of 42CrMo4 steel. Its preheating performed by preliminary laser passes should prevent cracks in the deposit, however all the trials were unsuccessful showing the high level of stresses reached during the process as cracks appeared at the fifth layer deposition (extremities of the substrate-clad interface). Table 1 gives the process parameters for the manufacturing of the simulated case. Figure 1a shows the sample geometry and thermocouple positions (top scheme). The final thin wall of (40*4.6*1.5) mm³ is centred on the substrate top surface.

Table 1 Process parameters used to generate the simulated sample.

	Substrate pre-heating	Clad deposition
Length of centered laser pass for pre-heating (mm)	40	40
Laser beam speed (mm/s)	41.7	8.3
Laser power (W)	260	500
Temperature at thermocouple P1 at preheating end and at cladding start in °C	217	134
Number of laser passes	20	10

The thermo-physical properties of the clad were measured by He pycnometry, dilatometry, differential scanning calorimetry DSC and laser flash analysis LFA from solid to liquid state. The thermal conductivity is computed from previous results. The liquidus temperature used in the FE model, i.e. 1653K, is obtained from thermo-dynamical simulations under para-equilibrium conditions for the first cellular solid phase.

Compression tests on small cylinders (8 mm diameter, 10 mm height) were performed with a Schenck 400 kN machine coupled with a quad elliptical radiant furnace 4x2000

W. The samples were extracted from a bulk deposit produced by laser cladding. The test results (strain rates from $2x10^{-3}$ to 50 $x10^{-3}$ s-1) justified the use of an elasto-plasic law as a low viscous effect was observed. Table 2 synthesizes the M4 material parameters used.

Table 2 M4 Temperature dependent thermal and mechanical properties of M4.

	Yield stress (Pa)	Young modulus (Pa)	Conductivity W/m.K	Apparent Thermal capacity J/kg.K	Dilatation coefficient m/m/°c
20 °C	1.65E+09	2.16E+11	18.57	460	5.11E-06
300 °C	1.65E+09	1.86E+11	18.72	440	5.45E-06
500 °C	1.20E+09	1.32E+11	19.40	480	5.20E-06
950 °C	1.4E+08	5.10E+10	26.86	595	5.89 E-06

The substrate properties first relied on previous tests performed on 42CrMo4 grade in Bainitic-Martensitic state, however a closer look at the material certificate identifies a pearlitic state which justifies the use of properties of [11]. This modification was a key point to be able by simulations to recover thermal fields measured during substrate pre-heating, showing the high sensitivity to thermo-physical properties.

3. Simulations and discussion

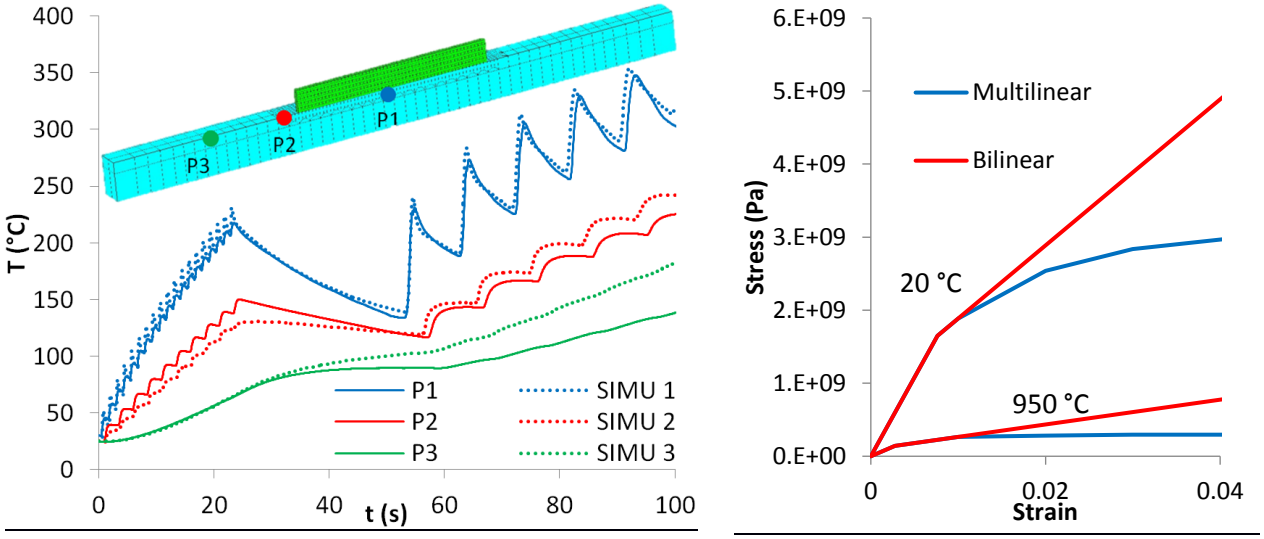

a) b)

Figure 1. a) Predicted and measured temperatures for 3 thermocouples (Pi), full lines and dotted lines respectively correspond to measurements and numerical results; b) Stress strain curves for bilinear and multilinear hardening cases at two different temperatures (the multilinear case is close to experimental values).

The details of the 3D thermal FE model can be found in [12], it is extended here to a thermo-mechanical analysis. The thermal histories measured and predicted within the substrate (Figure 1a) during preheating and cladding validate the FE results. The laser absorption, convection and radiation coefficients were respectively identified as constants, 0.42, 4.7 W/m².K and 0.6. The experimental hardening behaviour was either modelled by one line or by multilinear linear approximation (Figure 1b). Figure 1a shows

the positions P1 and P2 where the stress history is analysed. Figure 2a and b provide the Von Mises stress values until the fifth layer when cracks appeared assuming an annealing temperature of 800K or no annealing.

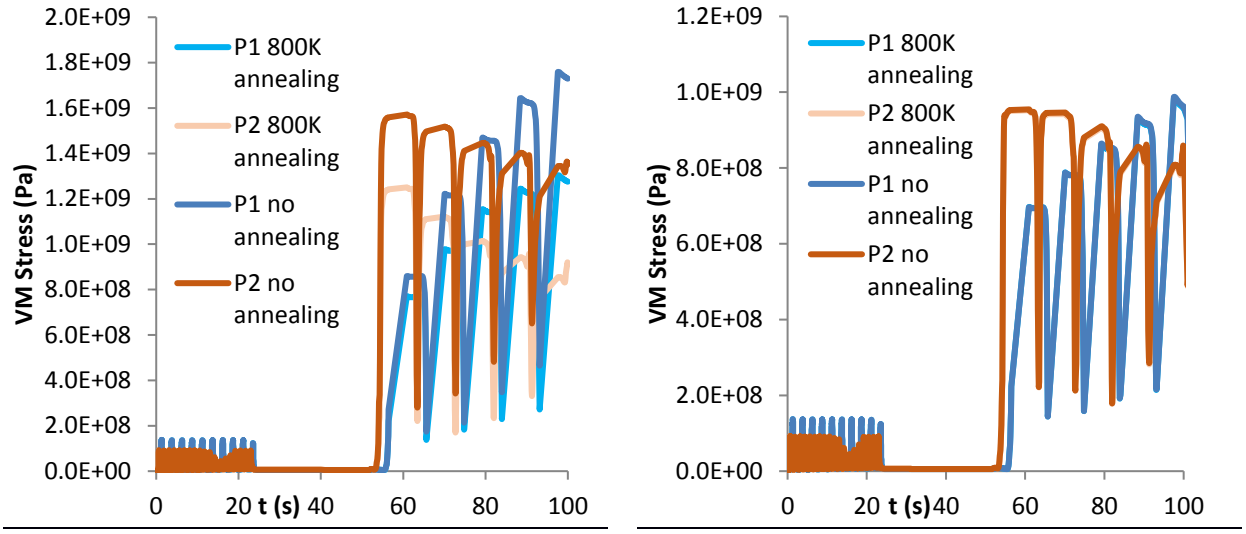

Figure 2. Von Mises stress for the bilinear a) and multilinear b) case with annealing temperature of 800K and without annealing. Points P1 and P2 are defined in Figure 1a

When accurate hardening model is used for this material, annealing temperature of 800K has no effect as the curves are superposed (see Figure 2b), while it strongly affects the predictions if high hardening slope is used. As the cracks release the stress field, no reproductive measurement of residual stresses allows the validation of stress predictions. New samples with 5 mm thick substrate and optimal preheating avoid cracks. Their residual stress fields are currently measured by X-Ray. They will allow the validation of the predicted residual stress field.

Acknowledgement: As FNRS F.R.S. Research director A/M. Habraken thanks this Fund for its financial support and all authors acknowledge its financial support for the PDR Laser Cladding grant.

4. References

[1] Boccalini M., Goldenstein H. (2001), Int. Mater. Rev. 46 92–115.
[2] Lewis, G.K., Schlienger, E., (2000), Mater. Des. 21, 417–423.
[3] Gockel, J., Beuth, J., Taminger, K., 2014. Addit. Manuf. 1–4, 119–126.
[4] Chiumenti, M., Lin, X., Cervera, M., Lei, W., Zheng, Y., Huang, W., 2017 Rapid Prototyp. J. 23, 448–463.
[5] Jardin R.T., Tchoufang Tchuindjang J., Duchêne L., Tran H.-S., Hashemi N., Carrus R., Mertens A., Habraken A.M. (2019) Materials Letters. 236:42-45
[6] Ye, R., Smugeresky, J.E., Zheng, B., Zhou, Y., Lavernia, E.J., 2006 Mater. Sci. Eng. A 428, 47–53
[7] Heigel J.C.C., Michaleris P., Reutzel E.W.W. (2015), Addit. Manuf. 5:9-19.
[8] Chapter 20 " Inelastic Mechanical Properties" . Abaqus 6.10 Analysis User's Manual
[9] E.R. Denlinger, P. Michaleris, Addit Manuf, 12 (2016), pp. 51-59
[10] Liang Wang, Sergio D. Felicelli, Phillip Pratt, Mater. Sci. Eng. A, 496, 234-241,
[11] http://www.aciers-premium.fr/images/filedownloads/fichestechniques/42CD4.pdf
[12] Tran, H.-S., Tchuindjang, J.T., Paydas, H., Mertens, A., Jardin, R.T., Duchêne, L., Carrus, R., Lecomte-Beckers, J., Habraken, A.M. (2017) Mater. Des. 128:130-142.